

Multi-Source Spatial Entity Linkage

Suela Isaj, Torben Bach Pedersen, *Senior Member IEEE*, and Esteban Zimányi

Abstract—Besides the traditional cartographic data sources, spatial information can also be derived from location-based sources. However, even though different location-based sources refer to the same physical world, each one has only partial coverage of the spatial entities, describe them with different attributes, and sometimes provide contradicting information. Hence, we introduce the spatial entity linkage problem, which finds which pairs of spatial entities belong to the same physical spatial entity. Our proposed solution (*QuadSky*) starts with a spatial blocking technique (*QuadFlex*) that creates blocks of nearby spatial entities with the time complexity of the quadtree algorithm. After pairwise comparing the spatial entities in the same block, we propose the *SkyRank* algorithm that ranks the compared pairs using Pareto optimality. We introduce the *SkyEx*-* family of algorithms that can classify the pairs with 0.85 *precision* and 0.85 *recall* for a manually labeled dataset of 1,500 pairs and 0.87 *precision* and 0.6 *recall* for a semi-manually labeled dataset of 777,452 pairs. Moreover, our fully unsupervised algorithm *SkyEx-D* approximates the optimal result with an *F-measure* loss of just 0.01. Finally, *QuadSky* provides the best trade-off between *precision* and *recall* and the best *F-measure* compared to the existing baselines.

Index Terms—spatial data, entity resolution, spatial blocking, skyline-based.



1 INTRODUCTION

WEB data and social networks are growing in terms of information volume and heterogeneity. Almost all online sources offer the possibility to introduce locations (geo-tagged entities accompanied by semantic details). A specific type of sources is *location-based sources*, whose primary focus is locations. In contrast to cartographic data sources, locations in location-based sources have a hybrid form that stands between a *spatial object* and an *entity*. We refer to them as *spatial entities* since they are spatially located but also identified by several other attributes such as the name of the location, the address, the phone, keywords, etc. Given that spatial entities are richer in terms of semantics, several systems that rely on spatial information such as geo-recommender systems, selecting influential locations, search engines that use geo-preferences, etc. could improve further their results by using spatial entities instead of spatial objects. Hence, it is of interest to collect and integrate spatial entities from location-based sources.

While a spatial object is identified only by the coordinates, this is not the case for spatial entities. Different spatial entities might co-exist in the same coordinates (shops in a shopping mall), or the same entity might be located in different but nearby coordinates across different sources. The identity of a spatial entity is the combination of several attributes. Nevertheless, the identity of a spatial entity is sometimes difficult to infer due to the inconsistencies in the sources; each location-based source contains different attributes; some attributes might be missing and even contradicting. For example, the spatial entity “Lygten” is

located in (57.436 10.534) and associated to keywords such as “coffee”, “tea”, and “cocoa and spices” in source A. In the meantime, source B contains the spatial entity named “Restaurant Lygten” in (57.435 10.533), described by the keyword “restaurant”. We need a technique that can automatically decide whether these two spatial entities are the same real-world entity. The problem of finding which spatial entities belong to the same physical entity is referred to as *spatial entity linkage* or *spatial entity resolution*. According to [33], entity linkage establishes a link between spatial entities, whereas entity resolution goes further by merging related entities into one merged representative entity. Since we do not perform the latter, we prefer the term entity linkage.

There are several works that apply entity linkage in various fields [2–5, 5, 6, 6, 9, 11, 12, 42] but little regarding spatial entities [18–20]. The entities in the majority of the existing related work on entity linkage refer to people; thus, the methodologies and the models are based on the similarities that two records of the same individual would reveal. Moreover, these works do not address the spatial character of spatial entities. As for the works in spatial entity integration [18–20], their main contribution is a tool rather than an algorithm. What is more, the methods propose arbitrarily attribute weights and score functions without experimentation nor evaluation. To sum up, *with the growing amount of information from location-based sources and the necessity for richer spatial information, a method to link spatial entities across different sources is needed.*

In this paper, we address the problem of spatial entity linkage across different location-based sources. First, we propose a method that uses the geo-coordinates to arrange the spatial entities into blocks. Then, we pairwise compare the attributes of the spatial entities. Later, we rank the pairs according to their similarities using our novel technique, *SkyRank*. Finally, we introduce three approaches (*SkyEx-F*, *SkyEx-FES*, *SkyEx-D*) for deciding whether the pairs of compared entities belong to the same physical entity. Our

- Suela Isaj and Torben Bach Pedersen are with the Department of Computer Science, Aalborg University, Selma Lagerlöfs Vej 300, 9220 Aalborg Øst, Denmark
E-mail: {suela, tbp}@cs.aau.dk
- Esteban Zimányi is with the Department of Computer and Decision Engineering, Université libre de Bruxelles, Avenue Franklin Roosevelt 50, 1050 Bruxelles, Belgium
E-mail: ezimanyi@ulb.ac.be

contributions are:

- 1) We introduce *QuadSky*, a technique for linking spatial entities and we evaluate it on real-world data from four location-based sources.
- 2) We propose an algorithm called *QuadFlex* that organizes the spatial entities into blocks based on their spatial proximity. *QuadFlex* inherits the concept and the complexity of quadtrees but avoids assigning nearby points into different blocks.
- 3) To rank the pairs by their similarity, we propose a flexible technique (*SkyRank*) that is based on the concept of Pareto optimality and needs no weights, nor scoring functions.
- 4) To decide whether a pair of spatial entities refers to the same physical entity or not, we propose the *SkyEx-** family of algorithms that considers the ranking order of the pairs and fixes a cut-off level to separate the classes.
- 5) We introduce two threshold-based algorithms: *SkyEx-F* that uses the *F-measure* to separate the classes, and *SkyEx-FES*, an optimized version of *SkyEx-F*, which provides a theoretical guarantee to prune 80% of the skyline explorations of *SkyEx-F*.
- 6) We propose *SkyEx-D*, a novel algorithm that is fully unsupervised and parameter-free and separates the classes based on their distance.

The remainder of the paper is structured as follows: first, we describe and compare to state of the art in Section 2; then, we introduce our proposed approach in Section 3; later, we detail the main stages of our approach: the spatial blocking in Section 4, comparing the pairs pairwise in Section 5, ranking the pairs based on their similarity and assigning them to a skyline in Section 6, and estimating the k^{th} level of skyline that best separates the classes in Section 7; after, we provide experiments regarding the performance of our proposed solution in Section 8 and finally, we conclude in Section 9.

2 RELATED WORK

The general data integration problem covers three aspects: *schema matching*, *entity resolution* and *data fusion* [1, 5]. In this section, we describe some works on *entity resolution*, *spatial data integration*, and we focus specifically on *spatial entity linkage*, which is applicable to our problem.

Entity resolution. The *entity resolution* problem has been referred in the literature with multiple terms including *deduplication*, *entity linkage*, and *entity matching*. Entity resolution has been used in various fields such as matching profiles in social networks [2], bioinformatics data [3], biomedical data [41], publication data [5, 6], genealogical data [4], product data [5, 6], etc. The attributes of the entities are compared, and a similarity value is assigned. The decision of whether to link two entities or not is usually based on a scoring function. However, finding an appropriate similarity function that combines the similarities of attributes and decides on whether to link or not the entities is often difficult. Several works use a training set to learn a classifier [9–11], others base the decision on a threshold derived through experiments [12, 13]. Other approaches that deal with uncertainty are described in the survey of Magnani and Montesi [7], including probabilistic, rule-based probabilistic, fuzzy,

and preference-based relationships between records as well as aggregation of multi-matches. Finally, the decision on whether to link to entities or not can also be based on the feedback of an oracle [5, 6] or of a user [6].

Spatial data integration. There are several works on integrating purely spatial objects. Spatial objects differ from spatial entities mainly because a spatial object is fully determined by its coordinates or its spatial shape whereas a spatial entity, in addition to being geo-located, has a well-defined identity (name, phone, opening hours, categories). The works on spatial object integration aim to create a unified spatial representation of the spatial objects that come from single/multiple sources. The solutions in [15, 16, 37, 38] are purely spatial and discuss the integration of spatial objects originating from sensors and radars to have a better representation of the surface in 2D or even in 3D. Road network integration is tackled by Schafers et al [17] where rules are used to detect matching and non-matching roads. The matching is performed on the similarity of the roads in terms of the length, angles, shape, as well as the name of the street if available. Nonetheless, this approach is based on roads only and cannot apply to the linking of spatial entities.

Spatial entity linkage. Accommodating the challenges of spatial entities for the entity resolution problem has been specifically addressed in [18–20, 39, 40, 44]. The work in [39] is a bridge between the works in spatial data integration and spatial entity linkage because the entities have names, coordinates, and types but similarly to spatial objects, they refer to landscapes (rivers, deserts, mountains, etc.). The method used in [39] is supervised and requires labeled data. Moreover, even the similarity of the attribute “type” is learned through a training set. Regarding [18–20], the main contribution of these works relies on designing a spatial entity matching tool rather than an integration algorithm. The authors of [20] provide a general matching technique for spatial entity matching. Spatial entities within a radius are compared with each other, and the value of the radius is fixed depending on the type of spatial entity. For example, the radius is 50 m for restaurants and hotels, but 500 m for parks. All attributes (except coordinates) are compared using the Levenshtein similarity. Since the name, the geodata and the type of the entity are always present, they carry two-thirds of the weight in the scoring function whereas the weights of the website, the address and the phone number are tuned to one-third. The prototype of the spatial entity matching in [19] relies on a technique that arbitrarily uses an average of the similarity scores of all textual attributes without providing a discussing on this choice. Similarly to [18, 19], the main contribution of the work in [20] is designing a tool for spatial entity integration. The underlying algorithm considers spatial entities that are 5 m apart from each other and compares the name of the entities syntactically and the metadata related to an entity semantically. Finally, the decision is taken using the belief theory [40]. The works in [18–20] lack an evaluation of the algorithms.

The present paper significantly extends a previous conference paper [44]. Specifically, contributions 5 and 6 are new, and 3 and 4 are improved compared to [44]. First, we modify the original *SkyEx* in [44] as to only rank and

not label the pairs, and we refer to it as *SkyRank*. Then, we delegate the classification problem to the three new algorithms, namely *SkyEx-F*, *SkyEx-FES* and *SkyEx-D*. The labeling process in [44] is dependent on a parameter k , and the experiments attempt to fix k using *precision*, *recall* and *F-measure*. We formalize this rationale in our proposed *SkyEx-F* algorithm. We improve further by providing a theoretical guarantee that *SkyEx-F* can be stopped before exploring the whole dataset, and propose the optimized *SkyEx-FES* that prunes 80% of the skyline explorations of *SkyEx-F*. Furthermore, we introduce a novel approach for estimating the number of skylines (*SkyEx-D*), which is fully unsupervised and parameter-free and closely approximates the threshold-based versions (*SkyEx-F* and *SkyEx-FES*). In the present paper, we provide a new set of experiments for *SkyEx-FES* and *SkyEx-D*, and compare the results with *SkyEx-F*.

Summary. On the one hand, the general entity resolution approaches propose interesting solutions, but they do not consider the spatial character of a spatial entity. They do not deal with geographic coordinates and are designed to match entities that represent individuals (profiles in social networks, authors and publications, medical records, genealogical connections, etc.) or even linking species in nature. The proposed solutions for the former [entity resolution in individuals], either supervised or based on an experimental threshold, are learned on human entity datasets. One can not merely assume the resemblance of behaviors in a human entity dataset to a spatial entity one. The solutions in the latter [species in nature] are based on domain-specific algorithms that have little to no applicability in other fields. On the other hand, there is little specific work in spatial entities [18–20], mostly focusing on a tool for spatial data integration rather than on the algorithm. In all these works, the scoring function is chosen arbitrarily and no evaluation provided.

3 SPATIAL ENTITY LINKAGE

In this section, we introduce the problem definition and our overall solution.

3.1 Problem Definition

The basic concept used in this work is a *spatial entity*, which includes locations, places, businesses, etc. Spatial entities originate from location-based sources such as directories with location information (yellow pages, Google Places, etc.) and location-based social networks (Foursquare, Gowalla, etc.).

Definition 1. A *spatial entity* s is an entity identified uniquely within a source I , located in a geographical point p and accompanied by a set of attributes $A = \{a_i\}$.

The attributes connected to an s can be categorized as:

- *Spatial*: the point where the entity is located, expressed in longitude and latitude.
- *Textual*: attributes that are in the form of text such as name, address, website, description, etc.
- *Semantic*: attributes in the form of text that enrich the semantics behind a spatial entity. Examples of this type are categories, keywords, metadata, etc.

- *Date, time or number*: other details about a spatial entity such as phone, opening hours, date of foundation, etc.

An example of a spatial entity originating from Yelp can be a place named “Star Pizza” in the point (56.716 10.114), with the keywords “pizza, fast food”, and with address “Storegade 31”. The same spatial entity can be found again in Yelp or other sources, sometimes having the same attributes, more, less or even attributes with contradictory values. Thus, there is a need for an approach that can unify the information within and across different sources in an intelligent manner.

Problem definition: Given a set of spatial entities S originating from multiple sources, the spatial entity linkage problem aims to find those pairs of spatial entities $\langle s_i, s_j \rangle$ that refer to the same physical spatial entity.

In the following section, we introduce *QuadSky*, our solution to the spatial entity linkage problem.

3.2 QuadSky Approach

We propose *QuadSky*, a solution based on a quadtree data partitioning and skyline exploration. The overall approach is detailed in Fig. 1. *QuadSky* consists of four main parts: spatial blocking (*QuadFlex*), pairwise comparisons, ranking the pairs (*SkyRank*), and labelling the pairs (the *SkyEx-** family of algorithms). S contains all spatial entities from all sources I . We propose *QuadFlex*, a quadtree-based solution that can perform the spatial blocking by respecting the distance between spatial entities and the density of the area. The output of *QuadFlex* is a list of leaves with spatial entities located nearby. Within the leaves, we perform the pairwise comparisons of the attributes.

After this second phase, we obtain a list of pairs of spatial entities and their similarities of attributes. We rank the pairs based on the skylines (concepts detailed in Section 6) using the *SkyRank* algorithm. In order to decide which pairs dictate a match and which not, we propose the *SkyEx-** family of algorithms (*SkyEx-F*, *SkyEx-FES*, and *SkyEx-D*) that finds which skyline level best separates the pairs that refer to the same physical spatial entity (the positives class) from the rest (the negative class). In the following sections, we detail each of the phases of *QuadSky*.

4 SPATIAL BLOCKING

Performing all possible comparisons between pairs of spatial entities is time-consuming. Since spatial proximity is a strong indicator in finding a match, the first step is to group nearby spatial entities in blocks. Several generic blocking techniques have been discussed in [27, 28], including methods based only on one attribute or several ones, block purging (discards the blocks that are over the size limit), etc. However, these techniques are mostly based on textual attributes and not applicable to spatial blocking. We propose a quadtree-based solution (*QuadFlex*) that uses a tree data structure but also preserves the spatial proximity of spatial entities. Our contribution is twofold; we use quadtrees (meant for spatial indexing) for spatial blocking, and we modify the recursive procedure of the quadtrees to accommodate more points that are nearby instead of splitting them arbitrarily in different children.

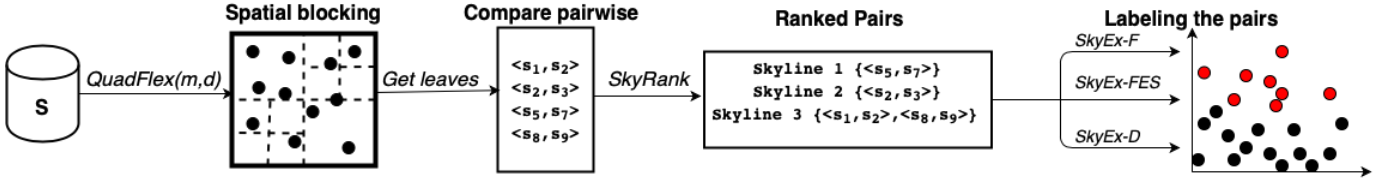


Fig. 1: QuadSky approach

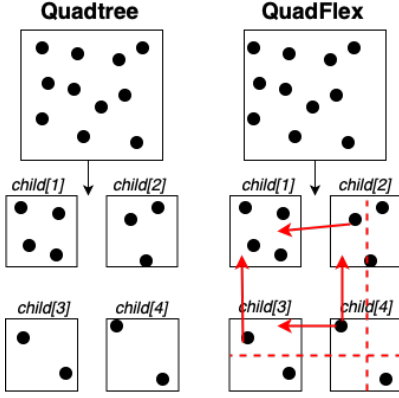


Fig. 2: QuadFlex versus quadtree

A quadtree is a tree whose nodes are always recursively split into four children when the capacity is filled [29]. Quadtrees of n points and d depth can be constructed in $O((d+1)n)$ time. After the quadtree is constructed, the points that fall in the same leaf are nearby spatially. Hence, these leaves are good candidates to be spatial blocks. There are several issues with the existing quadtree algorithm. First, a quadtree needs a capacity (number of points) as a parameter. The capacity is not a meaningful parameter for spatial blocking, while the density of the area is a better candidate. For example, if the area is too dense (e.g., city center), even though the capacity is not reached, a further split would be more beneficial. Spatial entities in the city center tend to be nearby, but they are more unlikely to refer to the same physical spatial entity. On the contrary, two points in the countryside (e.g., a farm) might be farther apart, but they still might be the same entity.

Second, a quadtree does not limit the distance between points. Even though two points might be in an area that respects the density, if they are quite distant from each other, it is not necessary to compare them. The maximal distance between two points in a child is the diagonal of the area (all quadtree children are rectangular). We used m , the diagonal of an area, as a parameter that controls the distance of points rather than comparing all distances between all spatial entities. Finally, a quadtree splits into four children, and sometimes nearby points might fall into different leaves. Hence, we might miss good pairs. We modify the procedure of the assignment of the points into a child by allowing more than one assignment.

Fig. 2 shows the modifications that we do to the construction of the traditional quadtree for our version *QuadFlex*. The traditional quadtree divides the area of each parent into four smaller areas, the children. A point belongs only

Algorithm 1 QuadFlex algorithm

Input: A set of entities $S = \{s_i\}$, diagonal m , density d

Output: The leaves QuadFlex Q $Q.leaves()$;

- 1: Create $Q(m, d)$ where Q has the dimensions of the bounding box of S
- 2: **for each** s in S **do**
- 3: $Q.insert(s)$ // Insert s into the QuadFlex
- 4: **end for**
- return** $Q.leaves()$

Method $insert(s)$

- 5: **if** $this.children \neq$ **then**
- 6: $Indexes \leftarrow getIndex(s)$ // Find where s belongs
- 7: **for each** i in $Indexes$ **do**
- 8: $this.child[i].insert(s)$ // Insert s to the children it belongs
- 9: **end for**
- 10: **end if**

- 11: **if** $this.diagonal > m$ **or** $this.density > d$ **then**
- 12: Split the current object $this$ into 4 children // The area is larger or denser than our restrictions, so split as in the traditional quadtree
- 13: **end if**

14: $Indexes \leftarrow getIndex(s)$

15: **for each** i in $Indexes$ **do**

16: $this.child[i].insert(s)$

17: **end for**

return

Method $getIndex(s)$

18: Let $vertical$ be the line that passes at 0.75 of the width of $this$

19: Let $horizontal$ be the line that passes at 0.75 of the height of $this$

20: **if** s is left of $vertical$ and above $horizontal$ **then**

21: $Indexes.add(1)$ // s fits in $child[1]$

22: **end if**

23: **if** s is right of $vertical$ and above $horizontal$ **then**

24: $Indexes.add(2)$ // s fits in $child[2]$

25: **end if**

26: **if** s is left of $vertical$ and below $horizontal$ **then**

27: $Indexes.add(3)$ // s fits in $child[3]$

28: **end if**

29: **if** s is right of $vertical$ and below $horizontal$ **then**

30: $Indexes.add(4)$ // s fits in $child[4]$

31: **end if**

return $Indexes$

to one child. In our modification, the area will split similarly to the quadtree, but when we assign a point to a child, we will consider including points that fall near the border also in the current child. For example, in Fig. 2, the red dashed line shows the area that will be considered to include points in the neighbors. We will add two points in $child[0]$, one coming from $child[1]$ and one from $child[3]$. Similarly, $child[1]$ and $child[3]$ will receive a point from $child[4]$.

Algorithm 1 details the procedure for retrieving the spatial blocks with *QuadFlex*. The algorithm creates the root of the *QuadFlex* tree with the bounding box of the data and parameters m and d (line 1). Then, it inserts each spatial entity into the *QuadFlex* (line 4) and finally returns its leaves. The methods $insert(s)$ and $getIndex(s)$ are self calls on the *QuadFlex* object ($this$). The insertion procedure is

similar to the traditional quadtree except that the constraint is not the capacity but the diagonal of the area m (maximal distance between points) and the density of the area d . Hence, if the diagonal of the QuadFlex is more than the distance m or the density is larger than our defined value d (line 12), the QuadFlex, similarly to a quadtree, will split into four children. However, in contrast to the traditional quadtree, a spatial entity might belong to more than one child. The method $getIndex(s)$ gets the list of indexes of the children where the new point will be assigned. Even though Q splits into 4 children, the lines *vertical* and *horizontal* (corresponding to the red dashed lines in Fig. 1) allow a logical overlap of the areas and thus, neighboring spatial entities will not be separated.

5 PAIRWISE COMPARISONS

After the spatial blocking, we perform a pairwise comparison of spatial entities that fall in the same leaf. Next, we describe the metrics for different types of attributes.

5.1 Textual Similarity.

We measure the textual similarity of spatial entities using the edit distance between the words. The Levenshtein distance [35] between string s_1 and string s_2 $d(s_1, s_2)$ is the number of edits (insertion, deletion, change of characters) needed to convert string s_1 to string s_2 . We define the similarity as:

$$TextSim(s_1, s_2) = \left(1 - \frac{d(s_1, s_2)}{\max(|s_1|, |s_2|)}\right) \quad (1)$$

Example 1. Let us consider "Skippers Grill" and "Skippers Grillbar". The Levenshtein distance to convert "Skippers Grill" to "Skippers Grillbar" is 3 (3 insertions). The lengths of the first and the second string are 14 and 17 respectively. So, $TextSim("Skippers Grill", "Skippers Grillbar") = 1 - (3/\max(14, 17)) = 0.8235$.

Note here that not all textual attributes can be handled similarly. String similarity metrics are usually appropriate for attributes like names, usernames, etc. Some other textual attributes require other metrics that need to be customized. In this paper, we consider address as a specific textual attribute. The similarity between two addresses cannot be measured with Levenshtein, Jaccard, Cosine, etc. since a small change in the address might be a giant gap in the spatial distance between the entities. For example, "Jyllandsgade 15 9480 Løkken" and "Jyllandsgade 75 9480 Løkken" have a distance of 1 and Levenshtein similarity of 0.963, but they are 650 meters apart. However, "Jyllandsgade 15 9480 Løkken" and "Jyllandsgade 15 9480 Løkken Denmark" have a distance of 8 and Levenshtein similarity of 0.772, but they are the same building. In [18, 19] the address is considered as another textual attribute without using its real semantics. In our case, we perform some data cleaning (removing commas, punctuation marks, lowercase, etc.), and then we search for equality ($s_1 = s_2$) or inclusion ($s_1 \subset s_2$ or $s_2 \subset s_1$). We assign a similarity of 1 in the case of equality and 0.9 in the case of inclusion. Otherwise, the strings are not considered the same.

5.2 Semantic Similarity.

The similarity of fields like categories, keywords or metadata cannot be compared only syntactically. Sometimes, several synonyms are used to express the same idea. Thus, we need to find a similarity than considers the synonyms as well. We use Wordnet [25] for detecting the type of relationship between two words and Wu&Palmer similarity measure (wup) [26], which calculates how related two words are by taking into account the depths of the two synsets (sets of synonyms) in WordNet, along with the depth of the Least Common Subsumer (the most specific concept that is an ancestor of both words). The semantic similarity between two spatial entities is the maximal similarity between their list of categories, keywords or metadata. The semantic similarity of the spatial entities s_1 and s_2 is:

$$SemSim(s_1, s_2) = \max\{wup(c_i, c_j)\} \quad (2)$$

where $c_i \in C_1$ and $c_j \in C_2$ and C_1 is the set of keywords of s_1 and C_2 is the set of keywords s_2 .

Example 2. Let us take an example of two spatial entities s_1 and s_2 and their corresponding semantic information expressed as keywords $C_1 = \{"restaurant", "italian"\}$ and $C_2 = \{"food", "pizza"\}$. The similarity between each pair is $wup("restaurant", "food") = 0.4$, $wup("italian", "food") = 0.4286$, $wup("restaurant", "pizza") = 0.3333$ and $wup("italian", "pizza") = 0.3529$. Finally, the semantic similarity of s_1 and s_2 is $SemSim(s_1, s_2) = \max\{0.4, 0.4286, 0.3333, 0.3529\} = 0.4286$.

5.3 Date, time or numeric similarity.

The similarity between two fields expressed as numbers, dates, times or intervals is simply a boolean decision (true or false). For example, if the phone numbers change with only one digit, they are still different. Even though the similarity of these fields relies only on an equality check, most of the effort is put in data preparation. For example, before the comparison, the different phone formats should be identified and cleaned from prefixes. Other data formats like intervals (opening hours) might require temporal queries for similarity, inclusion, and intersection of the intervals. In this paper, we do not use these attributes for measuring the similarity between spatial entities, but for constructing the ground truth.

Summary. Spatial entities are characterized by different spatial attributes that differ in formats but also in the semantics. Textual attributes are the most studied in the literature, and several similarity metrics have already been proposed. We use Levenshtein while comparing the names of spatial entities, and customized comparisons for the address. Thus, we check for equality or inclusion to detect similar addresses. Metadata, keywords, categories, etc. are attributes that carry semantics. Since textual similarity cannot measure the similarity between synonyms, we rely on Wordnet to detect similar keywords attached to the spatial entities. Finally, other formats such as numbers, intervals, timestamps, etc. can be checked for equality, but also some background knowledge might be needed to detect matches.

6 RANKING THE PAIRS

After the pairwise comparison, the pairs are represented as points in a space with n dimensions, where each dimension is an attribute. A pair has n similarity values, one for each attribute. We denote as δ_a the similarity of two spatial entities for attribute a . For example, a pair $\langle s_1, s_2 \rangle$ is represented as $\{\delta_{a_1}, \delta_{a_2}, \dots, \delta_{a_n}\}$. The problem that we need to solve is which $\langle s_i, s_j \rangle$ pairs indicate a strong similarity and should be considered for a match. This is an old problem in the entity linkage community. A classifier [9, 11, 31] can learn the behavior of the matches and detect the positive class. However, it is difficult to obtain labeled data, especially across different sources. Moreover, there is always the risk of overfitting when training a classifier on a sample. Some works assign weights on the similarity scores or put thresholds on each attribute similarity, and then test different combinations [12, 13, 31]. The problem that arises with these methods is that finding the best scoring function might require extensive experiments.

We propose a more relaxed technique that uses Pareto optimality [34] for filtering the positive class. A solution (x, y) is Pareto optimal when no other solution can increase x without decreasing y . The points in the same Pareto frontier or skyline have the same utility. Widely used in economics and multi-objective problems, Pareto optimality is free of weights and similarity score functions. In the context of entity resolution, the skylines provide a selection of points that are better than others, but without quantifying how much better. The pairs that refer to the same physical spatial entity (the positive class) are expected to have high values of δ . In general, the positive class is the minority and is spread all over the dataset, resembling outliers. This means that the first Pareto optimal frontier might contain only a couple of points (e.g. pairs with all $\delta(a_i) = 1$). Thus, an exploration of several skylines (k levels) is needed. Under the assumption that the best values of δ belong to the pairs from the positive class, we label the pairs up to the k^{th} skyline as the positive class and the rest as the negative. To the best of our knowledge, we are the first to propose a Pareto optimal solution for detecting matches for an entity linkage problem.

Definition 2. An attribute a is positive discriminating if its similarity δ_a indicates a positive class rather than a negative.

An example of a positive discriminating attribute is the similarity of name. A higher name similarity is more likely to indicate a match than a non-match. For example, the name similarity for *Mand & Bil* and *Mand og Bil* is 0.75, and for *Solid* and *Sirculus ApS* is 0.16. Hence, the former pair has a higher probability of being a match than the second. Examples of negative discriminating attributes are the edit distance between two names. If the distance between the names is high, then the pairs are less likely to be a match.

Definition 3. The utility of a positive discriminating attribute a , denoted as u_a , is the contribution of the attribute similarity δ_a to reveal a match, using Pareto Optimality ($\delta_a \xrightarrow{\text{Pareto Optimality}} u_a$).

Each attribute similarity contributes to the labeling problem. Intuitively, a higher similarity δ_a of a has a higher utility than a lower value of δ_a . Hence, if $\delta_a(\langle s_1, s_2 \rangle) > \delta_a(\langle s_3, s_4 \rangle)$, then $u_a(\langle s_1, s_2 \rangle) > u_a(\langle s_3, s_4 \rangle)$.

Definition 4. The utility of a pair denoted as $u(\langle s_i, s_j \rangle)$ is sum of the utilities of each of the attributes. $u(\langle s_i, s_j \rangle) = \sum_{i=1}^n u_{a_i}$.

Note that the utility of a pair is not the sum of the similarities of the attributes ($u(\langle s_i, s_j \rangle) \neq \sum_{i=1}^n \delta_{a_i}$) but the sum of their utilities ($u(\langle s_i, s_j \rangle) = \sum_{i=1}^n u_{a_i}$). Nevertheless, $u(\langle s_i, s_j \rangle) = \sum_{i=1}^n \delta_{a_i} = \sum_{i=1}^n u_{a_i}$ is a specific case.

Definition 5. A skyline of level k denoted as $Skyline(k)$ is the collection of pairs $\langle s_i, s_j \rangle$ of equal utility such that $u_{Skyline(k)} > u_{Skyline(k-1)}$.

Obviously, $Skyline(1)$ is the Pareto optimal frontier with the best values of δ_a . In order to continue with $Skyline(2)$, the points of $Skyline(1)$ are removed, and the frontier is calculated again. Every time we explore level k , the values in $Skyline(k)$ are the ones with the highest utility. This means that there is no other point in a lower level that can bring a higher utility to the positive class. This procedure continues until all the pairs are ranked according to their skyline. Algorithm 2 formalizes our proposed procedure Skyline Ranking (*SkyRank*) for ranking the pairs. The input is the set of pairs P produced from the *QuadFlex* blocking technique and the number of skyline levels k that we will explore. We find the points with the best combinations of δ that dominate the rest of the points and consequently, have a higher utility (line 3). Then, we put these points in P_k , which keeps the explored skylines and remove them from P (line 5). We stop when all the pairs are assigned to a skyline. Note that we have modified the original *SkyEx* in [44] as to only rank, not label the pairs. *SkyEx* in [44] is dependent on a parameter k that separates the positive from the negative class. In this paper, we provide methods to estimate the value of k in Section 7.

Algorithm 2 Skyline Ranking (SkyRank)

Input: A set of pairs $P = \{\langle s_i, s_j \rangle\}$
Output: A set of pairs and their skyline $P_k = \{\langle s_i, s_j \rangle, k\}$;
1: $P_k \leftarrow \emptyset$
2: **while** $|P_k| < |P|$ **do**
3: Filter $Skyline(k) = \{\langle s_i, s_j \rangle \mid \forall \langle s', s'' \rangle \in P - \{\langle s_i, s_j \rangle\}, u(\langle s_i, s_j \rangle) > u(\langle s', s'' \rangle)\}$ // Find the Skyline
4: Add $Skyline(k)$ to P_k // Move the skyline to P_k
5: $P = P - Skyline(k)$
6: **end while**
return P_k

After obtaining the ranking, we can assume that the pairs of the first few skylines are more likely to refer to the same physical entity than the rest, since they have the highest values of δ_a and thus, highest utility.

Assumption 1. The probability that a pair is labeled positive is inversely proportional to its skyline level.

More specifically, the assumption considers that for all $\langle s_i, s_j \rangle$ and $\langle s'_i, s'_j \rangle$ in P such that $\langle s_i, s_j \rangle \in Skyline(k)$, $\langle s'_i, s'_j \rangle \in Skyline(k')$ and $k < k'$, then $\langle s_i, s_j \rangle$ is more likely to be a match than $\langle s'_i, s'_j \rangle$. The assumption is intuitive, the more similar two pairs are, the more likely they are to be a match.

7 ESTIMATING K

In this section, we estimate k , the skyline level that separates the positive from the negative class. We differentiate

between two different methods for fixing the value of k : (i) *threshold-based*, which uses the labels of the dataset and selects the k that maximizes the F -measure (*SkyEx-F* and *SkyEx-FES*); (ii) *unsupervised*, which relies on the mean distance between the classes as an indicator to fix the value of k (*SkyEx-D*).

7.1 SkyEx-F and SkyEx-FES

This version of the *SkyEx* algorithm resembles a threshold-based method, where we have to find a value of k that separates the two classes. In contrast to the threshold-based methods used in entity resolution problems [13, 19, 20] where we have to find a threshold for each similarity of the attributes and then a threshold for the similarity function that aggregates the similarity scores, we have simplified our problem to only one parameter: k . We need to find the value of k that best separates the classes.

As a measure of a "good model", we choose to use the F -measure, given that our data tends to be unbalanced [45–47]. In the context of our problem, we define true positives TP as pairs that refer to the same physical entity and are correctly labeled as positives; true negatives TN as pairs referring to different physical entities and are correctly labeled as negatives; false positive FP as pairs that do not refer to the same physical entities but are wrongly labeled as positives; FN as pairs that refer to the same physical entity but are wrongly labeled as negatives. Thus, the precision is $p = \frac{TP}{TP+FP}$, the recall is $r = \frac{TP}{TP+FN}$ and F -measure ($F1$) = $2 \frac{p*r}{p+r}$.

Algorithm 3 SkyEx-F

Input: A set of pairs $P = \{(s_i, s_j)\}$
Output: A set of positive pairs P^+ and a set of negative pairs P^- ;
1: $P_k \leftarrow \emptyset, F \leftarrow \emptyset$
2: **while** $|P_k| < |P|$ **do**
 Lines 3-5 as Algorithm 2 ...
6: $P^+ \leftarrow P_k$
7: $P^- \leftarrow P$
8: Calculate $F1(k)$
9: Add $\langle k, F1(k) \rangle$ to F
10: **end while**
11: Find k^* such that $F1(k^*) = \max(F1(k_i)) \forall k_i \in \{1, |F|\}$
12: $P^+ \leftarrow \bigcup_{k_i=1}^{k^*} \text{Skyline}(k_i)$
13: $P^- \leftarrow P - P^+$
return P^+, P^-

The higher the k , the more unlikely it is for a pair in the k^{th} skyline to belong to the positive class (Assumption 1). *SkyEx-F* explores the first skylines and stops at the value of k that achieves the highest F -measure, which we refer as the *optimal* k , termed k^* . In order to find k^* , we use the same techniques as in Algorithm 2 for ranking the pairs, but we add some extra calculations within the loop (lines 6-9) and find the optimal k^* (line 11) in Algorithm 3. *SkyEx-F* calculates the F -measure for each skyline k by considering the pairs up to the k^{th} skyline as positive and the rest as negative. We add $F1(k)$ to the set F , which keeps track of the evolution of F -measure while exploring more skylines. We find k^* as the value of k that achieves the highest F -measure in F . The pairs from the first to the k^* level of skyline are labeled as positive and the rest as negative.

Note that *SkyEx-F* explores all the skylines and then, finds the threshold k . However, we can optimize Algorithm

3 by stopping at k^* before going through the full dataset P . In order to do this, we prove that while going deeper into skylines, the F -measure increases until an optimum point (or interval) and after that it cannot increase again. First, let us highlight some properties of p and r .

Property 1. *The recall is a monotonically non-decreasing function with respect to the number of skylines k .*

Proof. The recall after k skylines is $r(k) = \frac{TP(k)}{TP(k)+FN(k)}$. While we move to the next, $k+1^{\text{th}}$ skyline, we label more pairs as positive, so the probability of finding true positives TP is higher. Thus, $TP(k+1) \geq TP(k)$. As for the denominator, it is always the same despite the skyline level because the true positives are fixed in P and are independent of our labelling. This means that if we find more true positives (TP), then we automatically decrease the false negatives (FN). Hence, $TP(k+1) + FN(k+1) = TP(k) + FN(k)$. We can then show that $\frac{TP(k+1)}{TP(k+1)+FN(k+1)} \geq \frac{TP(k)}{TP(k)+FN(k)}$ so $r(k+1) \geq r(k)$. \square

Property 2. *Given Assumption 1, the precision is a monotonically non-increasing function with respect to the number of skylines k .*

The precision is $\frac{TP}{TP+FP}$. However, note that $TP + FP$ is what our algorithm labels as positive, which means all the pairs belonging to skylines up to the k^{th} level. Intuitively, considering Assumption 1, FP increase at a higher rate than TP while moving to higher k values. A formal proof of monotonic decreasing precision for systems that rank the results considering their relevance (like our skylines) can be found in [43].

Theorem 1. *The F -measure function with respect to the number of skylines k is increasing until an point or interval and after that it cannot increase again.*

Proof. Let us suppose that while moving deeper into the skylines, we found a peak point k or peak interval $[k_i, k_j]$ with $F1(k)$ as the corresponding F -measure. Note that for a peak interval the F -measure is constant. Since $F1(k)$ belongs to a peak point/interval, there exists a $F1(k+\epsilon)$ ϵ skylines after k such that $F1(k+\epsilon) < F1(k)$. Now, let us know suppose that we can find another optimum in $k+\delta$ such that $F1(k+\delta) > F1(k)$. Since $F1(k+\epsilon) < F1(k)$, consequently $F1(k+\delta) > F1(k) > F1(k+\epsilon)$. $F1 = 2 \frac{p*r}{p+r}$ can be rewritten as $F1 = \frac{2}{\frac{1}{p} + \frac{1}{r}}$. So, we can rewrite:

$$\frac{2}{\frac{1}{p(k+\delta)} + \frac{1}{r(k+\delta)}} > \frac{2}{\frac{1}{p(k)} + \frac{1}{r(k)}} > \frac{2}{\frac{1}{p(k+\epsilon)} + \frac{1}{r(k+\epsilon)}}$$

Using property 2, $p(k+\delta) \leq p(k+\epsilon)$, so:

$$\frac{2}{\frac{1}{p(k+\epsilon)} + \frac{1}{r(k+\epsilon)}} \geq \frac{2}{\frac{1}{p(k+\delta)} + \frac{1}{r(k+\epsilon)}}$$

which means that:

$$\frac{2}{\frac{1}{p(k+\delta)} + \frac{1}{r(k+\delta)}} > \frac{2}{\frac{1}{p(k+\delta)} + \frac{1}{r(k+\epsilon)}}$$

According the property 1, this inequality cannot hold, because $r(k+\delta) \geq r(k+\epsilon)$. Thus, our assumption of $F1(k+\delta) > F1(k)$ cannot hold and $F1(k)$ remains the highest value of F -measure. \square

Theorem 1 ensures that once we find the peak in the F -measure function, we can stop finding all the skylines and label the pairs accordingly. Consequently, we can allow Algorithm 3 to stop early. The modifications of Algorithm 3 are reflected in Algorithm 3a. We use the same procedure as in Algorithm 3 but we do not need to keep track of each of the skylines and their corresponding F -measures. Rather, we only keep the previous F -measures in $F_{previous}$. While moving to the next skyline, we calculate the F -measure and the first time we notice a drop (line 9), we stop the loop (line 10) and return both classes separated by the current k (lines 7-8). Otherwise, we update $F_{previous}$ to the current F -measure (line 12) and continue the search for the optimal k .

Algorithm 3a SkyEx-F Early Stop (SkyEx-FES)

Input: A set of pairs $P = \{(s_i, s_j)\}$
Output: A set of positive pairs P^+ and a set of negative pairs P^- ;

```

1:  $P_k \leftarrow \emptyset, F_{previous} \leftarrow 0$ 
2: while  $|P_k| < |P|$  do
    Lines 3-8 as Algorithm 3...
9: if  $F1(k) < F_{previous}$  then
10: break
11: else
12:  $F_{previous} \leftarrow F1(k)$ 
13: end if
6: end while
7:  $P^+ \leftarrow \bigcup_{k_i=1}^k \text{Skyline}(k_i)$ 
8:  $P^- \leftarrow P - P^+$ 
return  $P^+, P^-$ 

```

7.2 SkyEx-D

The methods described in the previous sections assume that the labels of the pairs are present. In this section, we assume no information about the labels and thus, we propose a heuristic for fixing the value of k . The heuristic is based on the distance between the positive and the negative class. We refer to the k discovered by *SkyEx-D* as *distance-based k* or k_d . In contrast to clustering, our classes are not characterized by a small intra-class distance. Various patterns can reveal a positive class; for example, a similar name but different category or similar category and similar address, etc. Thus, the positive pairs, positioned in the first skylines, are scattered and do not necessarily form a cluster. However, they can still be separated from the rest considering the distance to the negative class. Theoretically, the inter-class distance stays small when we are in the first skylines (potential positives), then starts to increase while we move into later skylines and finally falls again when we enter the deeper skylines (potential negatives). *SkyEx-D* notices the increase of the inter-class distance and sets k accordingly. In order to have an approximation of the inter-class distance, we use the mean and denote it as μ_d .

$$\mu_d = \frac{\sum d(p^k, p^{-k})}{|P_k|}$$

where $|P_k|$ is the number of pairs from the 1st to the k^{th} skyline, p^k is a pair in P^k , p^{-k} is a pair in $P - P^k$, and $d(p^k, p^{-k})$ is the distance between p^k and p^{-k} .

In order to fix k_d , we monitor the value of μ_d while moving deeper into the skylines. We denote by $\mu_d(k)$ the function of μ_d with regard to k . We use the first derivative of $\mu_d(k)$, denoted as $\mu'_d(k)$, to find the points where the $\mu_d(k)$

function decreases. The intuition behind this approach is that in the beginning the distance $\mu_d(k)$ starts increasing, which means that the first derivative has a positive slope ($\mu'_d(k) > 0$). Later, we enter the "grey area", where there is a mix of potential positives and potential negatives. This is where we need to stop, because we might lose in precision if we continue further. In order to find the "grey area", we note when the first derivative changes its slope to negative. In order to calculate $\mu'_d(k)$, we estimate the value of $\mu'_d(k)$ in each point k by the following formula:

$$\mu'_d(k) = \frac{\partial}{\partial k} \approx \frac{\mu_d(k+1) - \mu_d(k)}{1}$$

In order to not be sensitive to small fluctuations in $\mu'_d(k)$, we smoothen slightly $\mu'_d(k)$ with Gaussian function ($\frac{1}{\sigma\sqrt{2\pi}}e^{-(x-\mu)^2/2\sigma^2}$) using a small window. Then we monitor when $\mu'_d(k)$ decreases for the first time and we set k_d accordingly.

We modify Algorithm 2 to accommodate this approach. We calculate $\mu'_d(k)$ for each point of k in line 7. Then, we have to find the first negative value of the smoothened $\mu'_d(k)$ (line 9) and fix k_d accordingly (line 10). Finally, we return the classes defined by k_d in lines 16-17.

Algorithm 4 SkyEx-D

Input: A set of pairs $P = \{(s_i, s_j)\}$
Output: A set of positive pairs P^+ and a set of negative pairs P^- ;

```

1:  $P_k \leftarrow \emptyset$ 
    Lines 2-6 as Algorithm 2...
7: Calculate  $\mu'_d(k)$  in each  $k$ 
8: while  $k < k_{last}$  do
9:   if  $\text{smooth}(\mu'_d(k)) < 0$  then
10:      $k_d \leftarrow k$ 
11:   break
12:   else
13:      $k \leftarrow k + 1$ 
14:   end if
15: end while
16:  $P^+ \leftarrow \bigcup_{k_i=1}^{k_d} \text{Skyline}(k_i)$ 
17:  $P^- \leftarrow P_k - P^+$ 
return  $P^+, P^-$ 

```

Summary. Algorithm 4 estimates the skyline level k that best separates the positive class from the negative class. Similarly to clustering techniques that use heuristics to estimate their parameters, *SkyEx-D* uses the distance of the positive class from the rest as an indicator of class separability. However, in contrast to clustering metrics, which focus on the robustness of clusters, this is not a requirement for the *SkyEx-** family of algorithms. The positive pairs do not show similar patterns, but rather similar utilities, which can be better captured by skylines. Experimentally, we show that our inter-class distance approach estimates k_d very close to k^* without loosing in F -measure. In contrast to techniques that use a scoring function, the *SkyEx-** family of algorithms abstracts the concept of utility. Thus, no weights or similarity function is needed. Given that the points with a high utility are generally scattered, the *SkyEx-** family of algorithms can detect the positive class better than a clustering technique, which would fail in clustering together the positive class. Moreover, the flexibility of the *SkyEx-** family of algorithms makes it applicable to all problems where the expert knowledge on the contribution of the attributes is missing. Finally,

the *SkyEx*-* family of algorithms does not learn any behavior, so there is no risk of overfitting.

8 EXPERIMENTS

8.1 Dataset Description

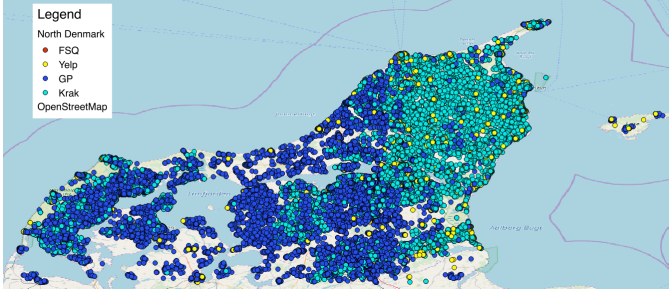


Fig. 3: North Denmark dataset

The spatial entities that will be used in these experiments originate from four sources, namely Google Places (GP), Foursquare (FSQ), Yelp, and Krak. Krak (www.krak.dk) is a location-based source that offers information about companies, enterprises, etc. in Denmark and is also part of Eniro Danmark A / S., which publishes The Yellow Pages. The data is obtained by using the available APIs and the algorithm detailed in [30]. The distribution of the spatial entities can be observed in Fig. 3. The dataset consists of 75,541 spatial entities where 51.50% comes from GP, 46.22% from Krak, 0.03% from FSQ, and 2.23% from Yelp. All the sources internally might contain possible links, so we need to compare entities within and outside the sources.

8.2 QuadFlex Performance

In this section, we compare the performance of our proposed blocking technique to the traditional quadtree and Fixed Radius Nearest Neighbors algorithm [36] (FNN). FNN finds the neighbors that fall within a fixed radius from each point. *QuadFlex* and the quadtree algorithm are implemented in Java, while FNN is run on a Postgres database (<https://www.postgresql.org>) using spatial indexes; more specifically, two spatial indexes: GiST (<https://www.postgresql.org/docs/current/gist.html>) (optimized C implementation of B-trees and R-trees) and SP-GiST (<https://www.postgresql.org/docs/current/spgist.html>) (optimized C implementation of quadtrees and k-d trees). Our original dataset contains 75,541 entities in the whole North Denmark region (around 16 towns, 7,933 km^2), so the density is not high. A high data density means more neighbors and consequently, more pairs to compare. In order to test our *QuadFlex* on different data densities, we simulate up to 1,000,000 random points from Aalborg (139 km^2).

Fig. 6 shows the comparison of quadtree, *QuadFlex* and FNN in terms of execution time (Fig. 6a) and number of comparisons (Fig. 6b). The FNN versions with data are computed on the database, and then the pairs are loaded back to the java implementation. The quadtree has the lowest execution time, followed by *QuadFlex*. FNN SP-GiST is comparable and sometimes even better than *QuadFlex* for small datasets. However, when the size of the dataset

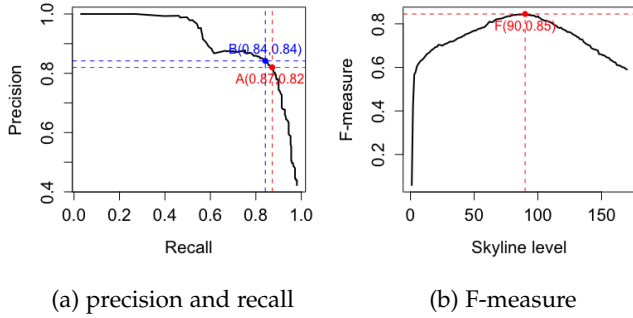
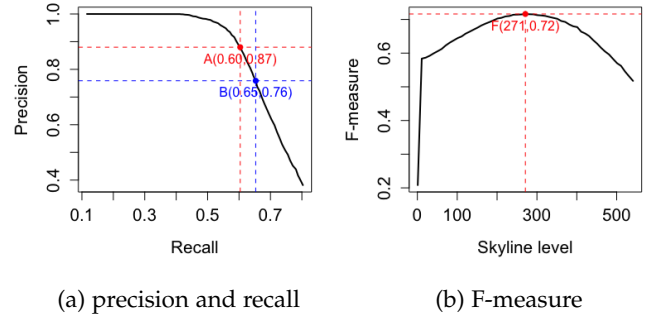
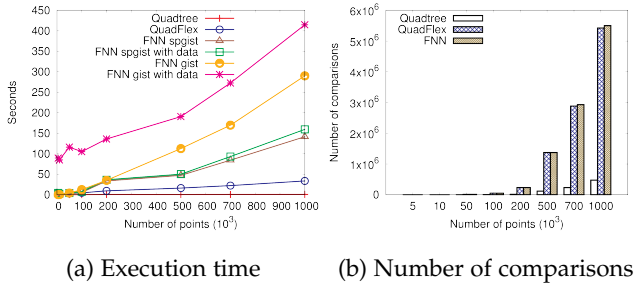
increases, *QuadFlex* manages to maintain an execution time that is eight times less than FNN GiST and 3 times less than FNN SP-GiST. FNN with SP-GiST index outperforms FNN GiST for all dataset sizes. As for the number of comparisons, *QuadFlex* enumerates 12 times more comparisons than quadtree, so our technique for not missing nearby pairs turned out effective. Moreover, *QuadFlex* contains almost all (99.99%) comparisons of FNN, compared to quadtree that contains only 10% of FNN. Furthermore, given that the scalability of *QuadFlex* is better than FNN, and *QuadFlex* is independent of the database implementations, the loss of around 0.01% of comparisons is insignificant. Moreover, this difference in comparisons can simply be explained by the fact that *QuadFlex* uses a rectangular area with diagonal of m meters, whereas FNN uses a circle with radius $\frac{m}{2}$. In the case of a square with diagonal m , the surface will be $\frac{m^2}{2}$, but for the circle with the diameter m the surface is $\pi \frac{m^2}{4}$. So, the surface of the circle is $\frac{\pi}{2}$ times more.

8.3 SkyEx-F results

We ran *QuadFlex* with 100 m and no density restriction, and we obtained 777,452 pairs. Having the same website or phone is a strong indicator of a match, so we use these attributes to infer the label. We refer to this labeling as *automatic labeling*. However, cases with different phone number or website but still the same entity, or same phone number but different entity might occur. For example, an entrepreneur who owns a fishing company and also a restaurant might use the same phone for both. Another example is the case of two different phones for the same entity on different sources. For this reason, we manually checked the labels of a sample of 1,500 pairs of entities, sometimes checking them even on maps and on the original sources. We will refer to the sample of manually checked pairs as D_{sample} and to the full dataset as D_{full} . Checking the labels manually on the full dataset of 777,452 pairs is unfeasible. Hence, we checked around 10,000 of the pairs, and for the rest, we rely on automatic labeling.

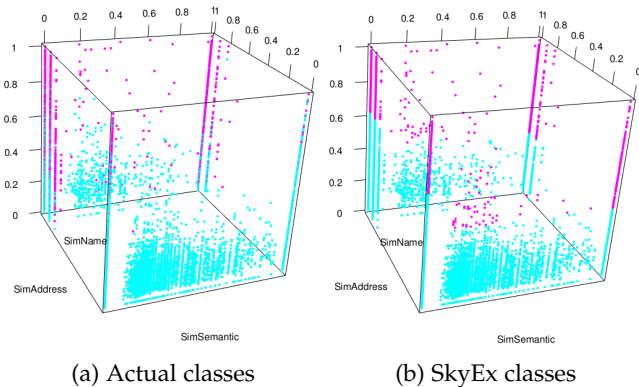
The results of *SkyEx-F* on D_{sample} and D_{full} are presented in Figs. 4 and 5. The curves in Figs. 4a and 5a shows the evolution of p (y -axis) and r (x -axis) while we move from one skyline to the next. As expected, *the more we explore, the more likely it is to retrieve more true positives and thus, improve the r* . However, *the more we explore and label pairs as positives, the more likely it is to increase the number of false positives, so the p degrades*. The algorithm explores several trade-offs; for example the points A and B are among the best. The point A with 0.87 p and 0.82 r in Fig. 4a is the same best point in terms of F -measure as well, so that is where *SkyEx-F* will fix k^* . Fig. 4b shows the levels of the skyline, and the value of F -measure achieved. The highest value is 0.85 that corresponds to $k = 90$.

The evaluation on the full dataset yields lower values compared to the sample, which might be a simple consequence of automatic labeling. Even though the labels are not all checked, p and r in D_{full} yield satisfactory values, e.g. points A and B , where A is with the highest F -measure of 0.72 is the result of *SkyEx-F* (Fig. 5b). A offers 0.6 r and 0.87 p while B offers a higher r of 0.65 but a lower p of 0.76. To have an idea of the real classes in D_{full} and the skyline, we

Fig. 4: SkyEx performance on D_{sample} Fig. 5: SkyEx-F performance on D_{full} 

(a) Execution time (b) Number of comparisons

Fig. 6: Comparing quadtree, QuadFlex and FNN



(a) Actual classes (b) SkyEx classes

Fig. 7: Positive (in pink) versus negative (in sky blue) classes for actual (a) and SkyEx-F (b) results

plotted their distribution in Fig. 7. Fig. 7a shows the actual positive classes in pink and the negative ones in sky blue. It is noticeable that the positive class pairs are allocated in the highest values of the dimensions. *SkyEx-F* with 271 levels (Fig. 7b) is able to capture this behaviour and achieve 0.6 r and 0.87 p . Despite the differences between both plots, *SkyEx-F* shows promising results in separating the positive class from the negative one.

8.4 Experimenting with Different QuadFlex Parameters

So far, we used *QuadFlex* blocking technique with 100 meters and no density restriction. In this section, we will evaluate our approach *QuadSky* for different blocking parameters.

Changing m , no density limit In this experiment, we test different values of m used in *QuadFlex* for creating

spatial blocks. We test m values of 1, 20, 40, 60, 80, and 100 meters. The size of the dataset for each of them is presented in Table 1. The spatially closeby points are likely to be a match. Hence, the percentage of the positive class is generally higher for smaller values of m . An interesting case is $m = 1$, where the percentage of the positive class is lower than $m = 20$. One would expect that points that are 1 meter apart would unquestionably be a match. However, this is not always the case. Shopping malls, buildings that host several companies, etc. are characterized by the same coordinates but not necessarily the same spatial entities.

Meters	1	20	40	60	80	100
Total	41053	118437	226331	372553	557421	777452
% of pos	17.11%	19.88%	11.28%	7.06%	4.82%	3.49%

TABLE 1: Dataset characteristics for different m

The results for different values of m are presented in Fig. 8. The point A is the value with the highest F -measure ($F1$). For all cases, the r is higher than 0.6. The p is higher than 0.8 for all values of m , except $m = 1$, where the p is 0.67. For $m = 1$, the positive and negative class are mixed, thus *SkyEx* loses a bit in p . This is also an argument against the works that merge arbitrarily points that are 5 m apart. *Spatial proximity is not a definitive indicator of a match.*

Changing d , $m \leq 100$. The density is another parameter of *QuadFlex* that helps in creating smaller blocks in dense areas and larger ones in sparse areas. In this experiment, we test different values of density d and its effect on the results. The size of the dataset and the percentage of the positive class in Table 2. When the density is smaller, we force *QuadFlex* to split further and create smaller blocks. Thus, the number of pairs reduces. Note that, on the contrary, the percentage of positives increases. Indeed, further splits allow us to create better blocks containing a higher percentage of positives. However, when the density limit increases above $\frac{30s}{1000m^2}$, fewer and fewer blocks are split further, so the dataset size and the percentage of the positives do not vary significantly. The results after running *SkyEx-F* are presented in Fig. 9. In all the cases, the r stays above 0.61 and the p above 0.87. A slightly better p (0.88) and r (0.63) is achieved in the case of a density of $\frac{10s}{1000m^2}$ (the lowest parameter). From both experiments with *QuadFlex* parameters, we can conclude that *SkyEx-F* adapts very well in finding the correct

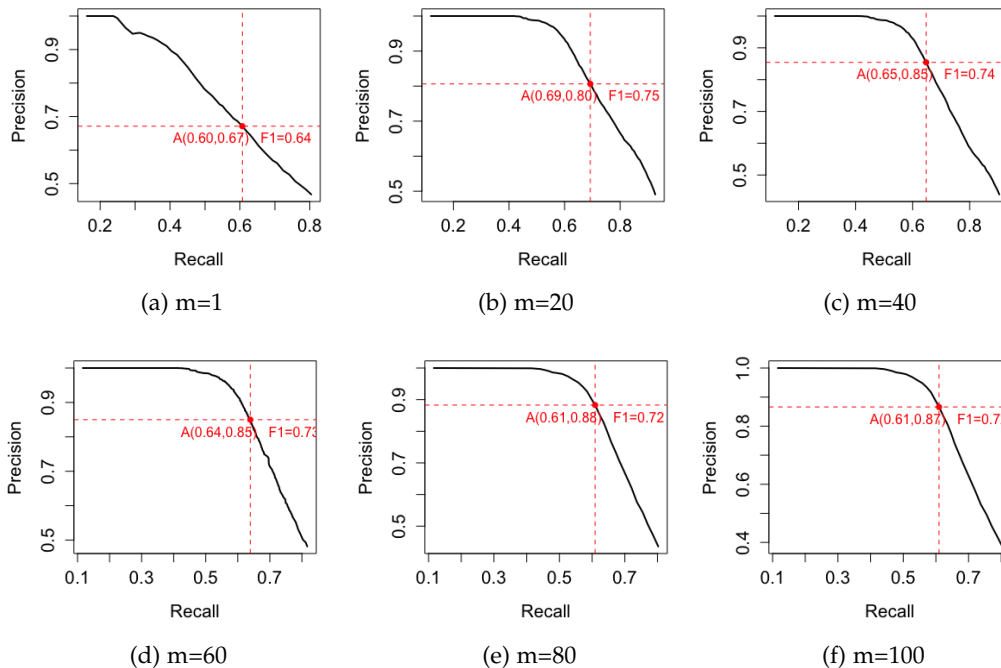


Fig. 8: Performance of SkyEx-F for different m , no density limit

classes even when the size of blocks change and even when the percentage of positives over negatives varies.

Den.	10s 1000m ²	20s 1000m ²	30s 1000m ²	40s 1000m ²	50s 1000m ²	60s 1000m ²
Total	290653	590583	711423	754195	770987	776664
% pos	8.61%	4.57%	3.81%	3.59%	3.51%	3.49%

TABLE 2: Dataset characteristics for different d

8.5 SkyEx-FES optimization

Given the theoretical guarantee in Theorem 1, we can stop *SkyEx-F* earlier as described in Algorithm 3a. We ran *SkyEx-FES* for spatial entities that are 30, 50, 80, and 100 m apart. For all the cases, *SkyEx-FES* found the same k^* values as *SkyEx-F* exploring only 27% of the skylines on average. The comparison regarding the number of iterations is shown in Table 3. For spatial entities that are 30 m, 50 m, 80 m, and 100 m apart, *SkyEx-FES* finds the optimal k exploring 36%, 27%, 23%, and 22% of the skylines, respectively. Moreover, our theoretical guarantee that the F -measure function has only one optimum can also be noticed in Fig. 4b and Fig. 5b.

Distance	30 m	50 m	80 m	100 m
<i>SkyEx-F</i>	1113	1182	1228	1228
<i>SkyEx-FES</i>	403	327	284	274

TABLE 3: Skyline explorations of *SkyEx-FES* compared to *SkyEx-F*

8.6 SkyEx-D performance

In these experiments, we consider the case of not having a labeled dataset and consequently, we cannot use the F -measure for fixing k . We use *SkyEx-D* (Algorithm 4) to set

k_d and evaluate our results in terms of F -measure. We apply *SkyEx-D* on spatial entities that are 30, 50, 80, and 100 meters apart.

According to Algorithm 4, after ranking the pairs by their skyline (Algorithm 2), we calculate the first derivative (μ'_d) in each point. The smoothed $\mu'_d(k)$ with respect to k are presented in Fig. 10. The red solid line shows the value of k^* (the k value with the highest F -measure), while the green dashed line represents k_d found by *SkyEx-D*. As specified in Algorithm 4, we note when the first derivative is negative for the first time and set k_d accordingly. In the case of spatial entities that are 30 m apart (Fig. 10a), k_d only 5 skylines apart from k^* , while for 50 m, there is a gap of 73 skylines between k^* and k_d .

These values of k_d are discovered using the first derivative as explained in Section 7.2. We illustrate the trend of μ_k while increasing k , which means that we explore deeper skylines and examine more pairs that are less likely to be a match. The distance from the positive class to the negative is smaller in the beginning because the mean μ_k is biased by the close points. While we increase k , μ_k increases, meaning that the classes are becoming more and more distinguishable from one another. The high values of μ_k show a high distance between the classes. For spatial entities that are 80 m and 100 m apart, μ_k starts dropping faster than for those that are 30 m and 50 m apart. This observation can be justified by the fact that closeby entities are more difficult to classify, so the "grey" area of the potential cut-off is larger. However, *SkyEx-D* detects the first decrease in μ_k from the first derivative and fixes k_d . Graphically, this point coincides with the beginning of the "grey" area.

Even though k_d is sometimes fixed far from k^* ($m=50$), the corresponding F -measures are almost the same. Fig. 12 shows the F -measure values for different k . The red line

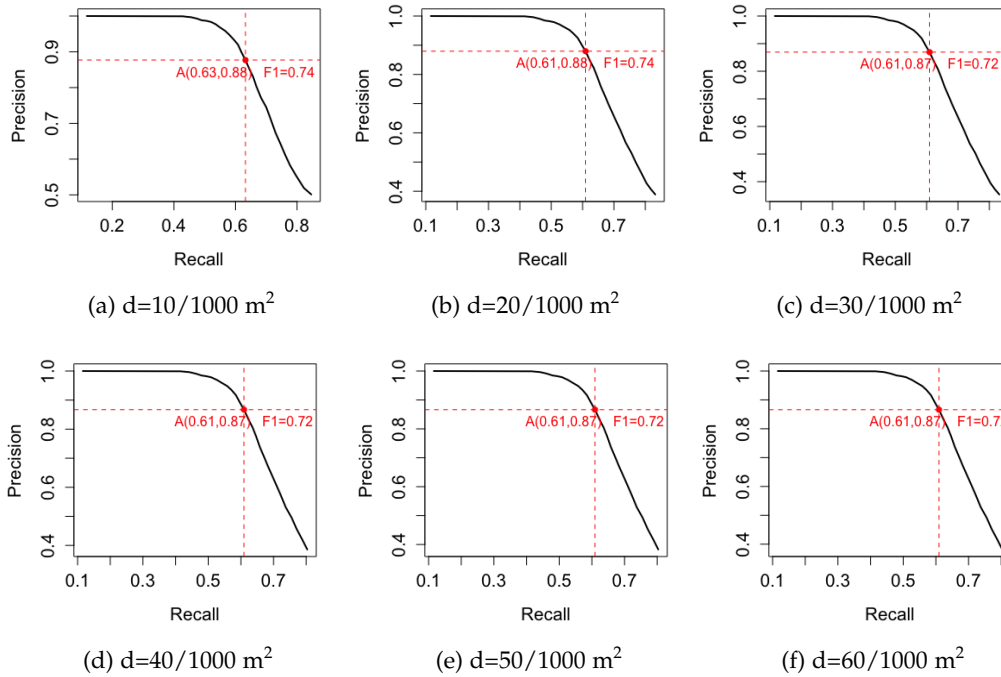


Fig. 9: Performance of SkyEx-F for different d , $m=100$

corresponds to k^* and the green line to k_d . The difference in F -measure is 0.002 for 30 m, 0.009 for 50 m, 0.002 for 80 m, and 0.004 for 100 m. Thus, *the difference in F -measure for the classifying the pairs using k_d instead of k^* is always less than 0.01*. This means that our *SkyEx-D*, even though fully unsupervised, is almost optimal in terms of F -measure.

8.7 Comparison with Baselines

Even though there are several papers in spatial data integration, the works of [18–20] are the most similar to ours, as the rest of the related work considers only spatial objects, not spatial entities, or uses supervised learning techniques. We will compare *QuadSky* to the following baselines:

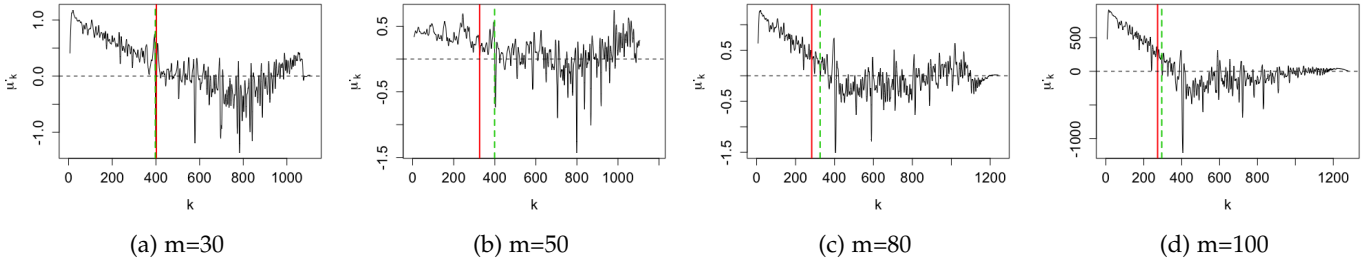
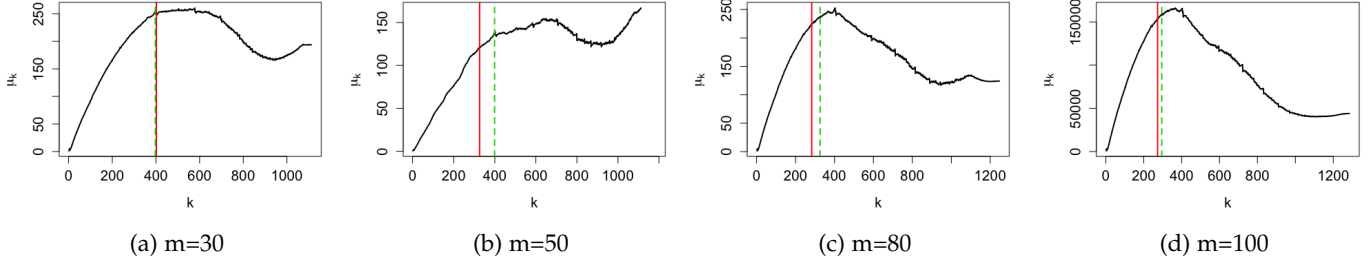
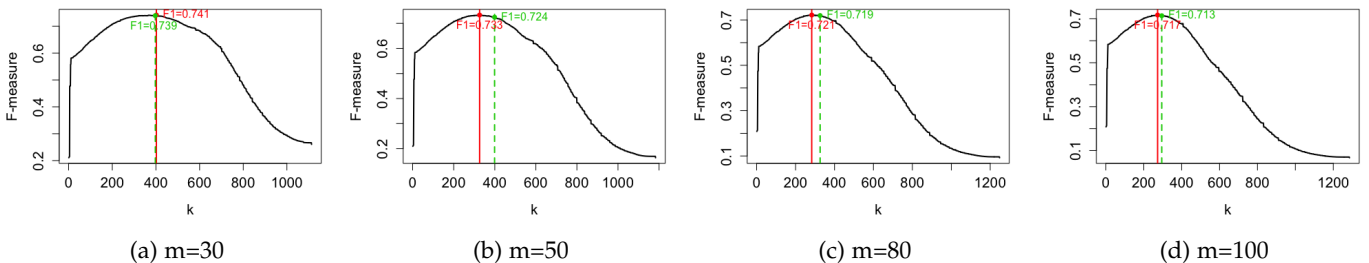
- 1) Berjawi et al.[19] propose Euclidean distance for the geographic coordinates and Levenshtein similarity for all other attributes. The similarities are integrated into a global similarity computed as a simple sum of the attribute similarities. The attributes mentioned in the paper are the name and the phone. However, since the phone is part of our automatic labeling, it can not be used in the algorithm as well. The authors consider pairs with $score \geq 0.75$ as a match with high confidence. We compare to this technique using name + address + geographic coordinates (V1) and name + geographic coordinates (V2).
- 2) Morana et al.[20] suggest filtering entities that share the same category or a token in the name. Then these entities are compared using the Euclidean distance for the coordinates, Levenshtein for the address and name, and Resnik similarity (Wordnet) for the category. Attributes like address, phone, etc. are considered secondary, so they are given $\frac{1}{3}$ of the weight in the similarity score function, while name, category and geographic prox-

imity carry $\frac{2}{3}$ of the weight. The authors show top k matches for each entity to the user to decide.

- 3) Karam et al.[18] starts with filtering spatial entities that are 5 m apart. Then, the similarity of the name is measured with Levenshtein distance, the geographic similarity with Euclidean distance, and the keywords are compared semantically. In order to decide which pairs to match and which not, the similarities are fused using belief theory [40].

The results using D_{full} and D_{sample} are presented in Table 4. In general, all the methods performed better in the manually labeled dataset D_{sample} due to the better quality of the labels. Berjawi et al.(V1)[19] has the highest p of above 0.93, but a poor r of at most 0.27 for both datasets and thus, a low F -measure of at most 0.43. It is actually expected, as Levenshtein similarity does not perform well with fields like address or phone, where a change in the digits makes a huge difference in the similarity of attributes. Berjawi et al.(V2)[19] yields reasonable results, the second best after *QuadSky*, with a p of 0.73 in D_{full} and 0.97 in D_{sample} , and a r of 0.56 in D_{full} and 0.60 in D_{sample} . The F -measure is 0.63 in D_{full} and 0.74 in D_{sample} . To compare with Morana et al.[20], we tried all values k from 1 to the maximal matches for a single point. The highest value of F -measure corresponded to a p of 0.39 and a r of 0.60. The behavior of Morana et al.[20] in D_{sample} is similar; the best value of F -measure was achieved for $k = 3$ and results are similar to those in D_{full} . The work of Karam et al.[18] achieves the highest r of 0.73 but a very low value of p of 0.23 for D_{full} . As a result, the F -measure is only 0.47. However, in D_{sample} , the method performs better overall (F -measure =0.6).

In comparison to all the baselines, both QuadSky versions provide the best trade-off between p and r , and thus, the highest F -measure in both datasets. In the case of D_{sample} , QuadSky

Fig. 10: Setting k_d using μ'_d Fig. 11: $\mu_d(k)$ function with respect to k Fig. 12: F -measure values for different k

with *SkyEx-F* and *QuadSky* with *SkyEx-D* achieve the best r compared to all baselines. What is more important, *QuadSky* with *SkyEx-D*, even using an unsupervised algorithm, is still better than the threshold-based baselines. The highest p values for both datasets is achieved by Berjawi et al.(V1)[19] but a very low recall and poor model performance overall. In fact, models that achieve extreme values (high precision-low recall or low precision-high recall) are not a viable solution because they are either too restrictive or too flexible, and their predictability is poor. Most of the current work base their scoring function on the assumption that the geographical proximity is essential, so besides spatial blocks, they include Euclidean distance in their similarity functions. *QuadSky* uses the spatial proximity for identifying candidates but not for making a decision. Berjawi et al. [19] (V2) assumes the same weights for all similarities, and the reported values of p and r are reasonable. However, the behaviors of the pairs can be of all types. *QuadSky* can capture these different behaviors better than a simple sum would.

9 CONCLUSIONS AND FUTURE WORK

Location-based sources provide rich information about spatial entities in terms of details and semantics. However,

Approach	D_{full}			D_{sample}		
	Prec.	Rec.	F1	Prec.	Rec.	F1
Berjawi et al.(V1)[19]	0.93	0.26	0.41	1.00	0.27	0.43
Berjawi et al.(V2)[19]	0.73	0.56	0.63	0.97	0.60	0.74
Morana et al.[20]	0.39	0.60	0.47	0.33	0.60	0.43
Karam et al.[18]	0.23	0.73	0.35	0.54	0.68	0.60
<i>QuadSky</i> with <i>SkyEx-F</i>	0.87	0.60	0.72	0.87	0.82	0.85
<i>QuadSky</i> with <i>SkyEx-D</i>	0.85	0.62	0.71	0.87	0.82	0.85

TABLE 4: Comparison with the baselines

identifying which pairs of spatial entities refer to the same physical entity across different sources is a challenging problem due to the lack of labeled data, data quality problems in the sources and the difficulty of coming up with a data-independent scoring function. In this paper, we addressed the problem of spatial entity linkage across multiple location-based sources. We proposed *QuadSky*, an approach that consists of a spatial blocking technique *QuadFlex*, pairwise comparisons with suitable similarity metrics for each attribute, a skyline-based ranking algorithm *SkyRank*, and the *SkyEx-** family of algorithms for classifying the pairs.

QuadFlex arranges the spatial entities into spatial blocks with a low execution time (4-8 times less than Fixed Radius Nearest Neighbors algorithm [36] (FNN)) and without missing relevant comparisons (99.99% of FNN comparisons).

The *SkyEx*-* family of algorithms solves the data labeling problem using Pareto optimality for ranking (*SkyRank*) and yields good results in terms of p and r . Moreover, due to its flexibility, the *SkyEx*-* family of algorithms better captures the behavior of pairs and outperforms the existing baselines in terms of F -measure. More specifically, *SkyEx-F* achieves 0.84 p and 0.84 r on a manually labeled dataset and 0.87 p and 0.6 r on an automatically labeled dataset. Our fully unsupervised algorithm *SkyEx-D* finds k_d number of skylines very close to the optimal k^* (an F -measure loss of just 0.01). In future work, we aim to study different blocking techniques that combine several attributes. Moreover, we plan to extend our *SkyEx*-* family of algorithms to general (non spatial) entity resolution problems. Furthermore, our goal is to identify better the "grey area" and propose methods to improve our results.

REFERENCES

- [1] X. L. Dong, and D. Srivastava. Big data integration *ICDE*, 2013
- [2] K. Shu, and S. Wang, and J. Tang, and R. Zafarani, and H. Liu. User identity linkage across online social networks: A review *ACM SIGKDD Explorations Newsletter*, 2017
- [3] C. T. Yui, and L. J. Liang, and W. J. Soon, and W. Husain. A survey on data integration in bioinformatics *ICIEIS* 2011,
- [4] J. Efremova, and B. Ranjbar-Sahraei, and H. Rahmani, and F. Oliehoek, and T. Calders, and K. Tuyls, and G. Weiss. Multi-source entity resolution for genealogical data, *Population reconstruction*, 2015
- [5] D. Firmani, and B. Saha, and D. Srivastava. Online entity resolution using an oracle *PVLDB*, 2016
- [6] R. Maskat, and N. W. Paton, and S. M. Embury. Pay-as-you-go Configuration of Entity Resolution *Transactions on Large-Scale Data and Knowledge-Centered Systems XXIX*, 2016
- [7] M. Magnani, and D. Montesi. A survey on uncertainty management in data integration, *JDIQ*, 2010
- [8] N. Ayat, and R. Akbarinia, and H. Afsarmanesh, and P. Valduriez. Entity resolution for probabilistic data, *Information Sciences*, 2014
- [9] M. Edwards, and S. M. Wattam, and P. E. Rayson, and A. Rashid. Sampling labelled profile data for identity resolution *BigData*, 2016
- [10] O. Peled, and M. Fire, and L. Rokach, and Y. Elovici. Entity matching in online social networks *SocialCom*, 2013
- [11] O. Goga, and H. Lei, and S. K. Parthasarathi, and G. Friedland, and R. Sommer, and R. Teixeira. Exploiting innocuous activity for correlating users across sites *WWW*, 2013
- [12] A. Panchenko, and D. Babaev, and S. Obiedkov. Large-Scale Parallel Matching of Social Network Profiles *AIST*, 2015
- [13] G. Quercini, and N. Bennacer, and M. Ghufuran, and C. N. Jipmo. LIAISON: reconciliation of Individuals Profiles Across Social Networks *Advances in Knowledge Discovery and Management*, 2017
- [14] L. Li, and J. Li, and H. Gao. Rule-based method for entity resolution *TKDE*, 2015
- [15] R. Abdalla Geospatial Data Integration *GeoICT*, 2016
- [16] PG Tabarro, and J. Pouliot, and R. Fortier, and L. Losier. A WebGIS to Support GPR 3D Data Acquisition: A First Step for the Integration of Underground Utility Networks in 3D City Models, *ISPRS*, 2017
- [17] M. Schäfers, and U. Lipeck. SimMatching: adaptable road network matching for efficient and scalable spatial data integration *ACM SIGSPATIAL PhD Workshop*, 2014
- [18] R. Karam, and F. Favetta, and R. Kilany, and R. Laurini Integration of similar location based services proposed by several providers *NDT*, 2010
- [19] B. Berjawi, and E. Chesneau, and F. Duchateau, and F. Favetta, and C. Cunty, and M. Miquel, and R. Laurini. Representing Uncertainty in Visual Integration. *DMS*, 2014
- [20] A. Morana, and T. Morel, and B. Berjawi, and F. Duchateau. Geobench: a geospatial integration tool for building a spatial entity matching benchmark *ACM SIGSPATIAL*, 2014
- [21] Ma Nentwig, and M Hartung, and A Ngonga Ngomo, and E. Rahm. A survey of current link discovery frameworks *Semantic Web*, 2017
- [22] A. Ngomo, and S. Auer. Limes-a time-efficient approach for large-scale link discovery on the web of data., *IJCAI*, 2011
- [23] J. Volz, and C. Bizer, and M. Gaedke, and G. Kobilarov. Silk-a link discovery framework for the web of data., *LDOW*, 2009
- [24] J. Euzenat, and A. Ferrara, and W. R. Van Hage, and L. Hollink, and C. Meilicke, and A. Nikolov, and F. Scharffe, and P. Shvaiko, and H. Stuckenschmidt, and O. Sváb-Zamazal, and others Final results of the ontology alignment evaluation initiative 2011, *OM*, 2011
- [25] C. Fellbaum WordNet *Theory and applications of ontology: computer applications*, 2010
- [26] Z. Wu, and M. Palmer Verbs semantics and lexical selection, *ACL*, 1994
- [27] G. Papadakis, and J. Svirsky, and A. Gal, and T. Palpanas. Comparative analysis of approximate blocking techniques for entity resolution, *PVLDB*, 2016
- [28] G. Papadakis, and E. Ioannou, and C. Niederée, and T. Palpanas, and W. Nejdl. Beyond 100 million entities: large-scale blocking-based resolution for heterogeneous data, *WSDM*, 2012
- [29] H. Samet The quadtree and related hierarchical data structures *CSUR*, 1984
- [30] S. Isaj, and T. B. Pedersen. Seed-Driven Geo-Social Data Extraction *SSTD*, 2019
- [31] H. Köpcke, and A. Thor, and E. Rahm Evaluation of entity resolution approaches on real-world match problems, *VLDB*, 2010
- [32] S. E. Whang, and D. Menestrina, and G. Koutrika, and M. Theobald, and H. Garcia-Molina. Entity resolution with iterative blocking *SIGMOD*, 2009
- [33] D. G. Brizan, and A. U. Tansel A. survey of entity resolution and record linkage methodologies *Communications of the IIMA*, 2006
- [34] Y. Censor. Pareto optimality in multiobjective problems *Applied Mathematics and Optimization*, 1977
- [35] V. Levenshtein. Binary codes capable of correcting deletions, insertions, and reversals, *Soviet physics doklady*, 1966
- [36] J. L. Bentley, and D. F. Stanat, and E. H. Williams Jr. The complexity of finding fixed-radius near neighbors *Information processing letters*, 1977
- [37] S. Balley, and C. Parent, and S. Spaccapietra. Modelling geographic data with multiple representations *IJGIS*, 2004
- [38] V. Walter, and D. Fritsch. Matching spatial data sets: a statistical approach, *IJGIS*, 1999
- [39] V. Sehgal, and L. Getoor, and P. D. Viechnicki. Entity resolution in geospatial data integration *GIS*, 2006
- [40] A. O. Raimond, and S. Mustière. Data matching—a matter of belief *Headway in spatial data handling*, 2008
- [41] P. Christen, and T. Churches, and M. Hegland. Febrl—a parallel open source data linkage system *PAKDD*, 2004
- [42] S. Isaj, and N. Seghouani, and G. Quercini. Profile Reconciliation Through Dynamic Activities Across Social Networks, *CAiSE*, 2019
- [43] M. Gordon, and M. Kochen. Recall-precision trade-off: A derivation *Journal of the American Society for Information Science*, 1989
- [44] S. Isaj, and E. Zimányi, and T. B. Pedersen. Multi-Source Spatial Entity Linkage *SSTD*, 2019
- [45] G. M. Weiss, and H. Hirsh. Learning to predict extremely rare events *AAAI workshop on learning from imbalanced data sets*, 2000
- [46] J. Zhang, and E. Bloedorn, and L. Rosen, and D. Venese. Learning rules from highly unbalanced data sets *ICDM*, 2004
- [47] D. A. Cieslak, and N. V. Chawla. Learning decision trees for unbalanced data *ECML PKDD*, 2008



Suela Isaj is a Ph.D. fellow at the Center for Data-Intensive Systems (Daisy) at Aalborg University, Denmark. She received an M.Sc. degree from the University of Tirana (2013) and a joint M.Sc. degree from Université libre de Bruxelles, Université François Rabelais and Centrale-Supélec (2017). Her current research is focused on location-based data extraction and integration, data mining, and data analytics.



Torben Bach Pedersen is a professor at the Center for Data-Intensive Systems (Daisy) at Aalborg University, Denmark. His research concerns Big Data analytics for on multidimensional Data. He is an ACM Distinguished scientist, a senior member of the IEEE, and a member of the Danish Academy of Technical Sciences.



Esteban Zimányi is a professor and the director of the Department of Computer and Decision Engineering (CoDE) at Université libre de Bruxelles. He is Editor-in-Chief of the Journal on Data Semantics published by Springer. His current research interests include data warehouses, spatio-temporal databases, geographic information systems, and semantic web.